Available online at www.sciencedirect.com
SCIENCE DIRECT
Journal of Photochemistry and Photobiology A: Chemistry 180 (2006) 184–188
Journal of Photochemistry and Photobiology A:Chemistry
www.elsevier.com/locate/jphotochem

TiO_2 nanorods as additive to TiO_2 film for improvement in the performance of dye-sensitized solar cells

Jong-Hyun Yoon [a], Song-Rim Jang [a], R. Vittal [a], Jiwon Lee [b], Kang-Jin Kim *

[a] *Division of Chemistry and Molecular Engineering, Korea University, Seoul 136-713, Republic of Korea*
[b] *Samsung SDI, Co. Ltd., Gyeonggi-Do, 449-577, Republic of Korea*

Received 28 June 2005; received in revised form 5 September 2005; accepted 18 October 2005
Available online 18 November 2005

Abstract

Anatase TiO_2 nanorods and nanotubes were produced from hydrolyzed $TiCl_4$ using an anodic alumina membrane (AAM) as template. SEM analysis indicated that the form of nanostructures depends on the pore size of the membrane, and their diameters are almost same regardless of nominal pore sizes. When the nanorods were incorporated at about 10 wt% level in a P25 TiO_2 film electrode of a dye-sensitized solar cell, its solar energy conversion efficiency was enhanced by about 42% as a result of a higher short-circuit photocurrent, compared with that of a cell fabricated with bare P25. The nanostructures were characterized by SEM, energy dispersive X-ray spectroscopy and Raman spectroscopy. Reasons for the invariance of sizes of nanostructures, and for the enhancement of the solar energy conversion efficiency are discussed. These explanations are supported by SEM, dye-adsorption measurements and light scattering findings.

Keywords: Anodic alumina membrane; TiO_2 nanostructure; Dye-sensitized solar cell; Short-circuit photocurrent; Solar energy conversion efficiency

1. Introduction

One of the ways of enhancing the surface area of nanocrystalline TiO_2 material is to convert it into nanotubes or rods, since these structures have larger surface areas than their particulate forms. The electronic properties of these structures also differ from those of TiO_2 nanocrystals used in dye-sensitized solar cells (DSSCs) [1]. From these points of view, this conversion is of relevance in DSSCs, where a high surface area of the TiO_2 film electrode is a prerequisite. It is also envisaged that the incorporation of such nanostructures in TiO_2 film can enhance light scattering and electron transfer in the film, which are also helpful for enhancing photocurrent. In addition, a high level of dye adsorption on the titania surface is expected due to the high aspect ratio of the nanostructure. Gracia et al. obtained the highest photo-response using a photoelectrochemical cell having an anatase film with columnar microstructure prepared by plasma enhanced chemical vapor deposition [2]. These factors prompted us to use TiO_2 nanostructure in a DSSC with the intension of improving the cell's performance.

AAMs have been widely used to prepare TiO_2 nanostructures, in different ways [3–6]. TiO_2 nanorods and tubes have been prepared by several groups using, e.g. block copolymer surfactants [7], templating polymer gels [8], heating-sol–gel template process [9], sol–gel coating of electrospun polymer fibers [10], template- and catalyst-free metalorganic chemical vapor deposition [11], chemical processing [12], electrochemical deposition [5], etc. We found only two cases where TiO_2 nanostructures have been used in solar cells [13,14]. Adachi et al. [13] and Ngamsinlapasathian et al. [14] used, as a major component, surfactant-assisted nanostructures of titania to prepare film electrodes for DSSCs.

In this paper, we report for the first time on the incorporation of well-defined TiO_2 nanorods at ca. 10 wt% level in the P25 film electrodes of DSSCs to enhance the solar energy conversion efficiency of the cells relative to a cell with a bare P25 film electrode. Preparations of different nanostructures, i.e. nanorods and nanotubes, depending on pore size of AAM, and almost the same size nanorods with one order difference in the pore size are novel aspects of this paper.

* Corresponding author. Tel.: +82 2 3290 3127; fax: +82 2 3290 3121.
E-mail address: kjkim@korea.ac.kr (K.-J. Kim).

1010-6030/$ – see front matter © 2005 Elsevier B.V. All rights reserved.
doi:10.1016/j.jphotochem.2005.10.013

2. Experimental

Twenty-two millilitres of $TiCl_4$ was dropped into 78 ml of chilled water (at ca. 4 °C) to produce a 2.0 M hydrolyzed stock solution. An AAM (Anodisc 13, Whatman) was used as a template. Three pore sizes of AAM, that is, 0.02, 0.1 and 0.2 μm were used, as appropriate. A hydrolyzed clear solution of 60 μl of 0.20 M $TiCl_4$ was loaded on the top surface of a piece of AAM placed on a filter paper within a porcelain crucible, and pores were filled by using an aspirator for 40 min at room temperature. The soaked membrane was placed vertically in a porcelain boat and heated in an oven for 2 h at 50 °C to accelerate the precipitation, which otherwise takes about 3 days at room temperature. The AAM was then dissolved away by immersion in a 1 M NaOH solution for 30 min. The resulting material was washed with distilled water and dried at 100 °C for 30 min. For Raman analysis, the product was further annealed at 450 °C for 30 min.

For photovoltaic experiments we selected nanorods produced using an AAM with 0.02-μm pore size. These nanorods were dispersed in distilled water and subjected to ultrasonic vibrations for about 3 min at 50 °C, before being mixed with P25 TiO_2. This process reduced their original sizes considerably. These fragmented nanorods were mixed with P25 at 5, 10 and 15 wt% to produce a 1.2 g composite. This was used to prepare a colloidal viscous solution as described previously [15]. This colloidal mixture was coated on fluorine-doped SnO_2 (FTO) conducting glass (Libbey–Owen–Ford Co.) using a doctor blade technique. The FTO to be coated with TiO_2 was fixed on a plain glass plate using two strips of tape. The film thickness was maintained in all cases at 12 ± 1 μm. TiO_2 film thickness was controlled by using different number of tape layers (~4 μm for one layer of tape). The TiO_2 slurry prepared with nanorods was placed on the FTO substrate and dragged in one direction using a doctor blade to produce a uniform TiO_2 film thickness. Longer nanorods can lie in horizontal position in the film, facilitating the maintenance of the film thickness to be the same. The film was then annealed at 450 °C for 30 min in air. The film thus obtained was then coated with dye in absolute ethanol (0.3 mM $[RuL_2(NCS)_2]\cdot 2H_2O$, where L = 2,2′-bipyridine-4,4′-dicarboxylic acid) for 24 h at room temperature. DSSCs were fabricated as reported previously [15]. The electrolyte solution consisted of 0.6 M 1,2-dimethy-3-hexylimidazolium iodide, 0.5 M 4-*tert*-butylpyridine, 0.1 M LiI and 0.05 M I_2 in 3-methoxypropionitrile.

A Hitachi S-4300 field emission-scanning electron microscope (SEM) was used to obtain nanostructure morphology and TiO_2 film thickness. Energy dispersive X-ray (EDX) spectra were recorded using the same instrument. Raman spectra were obtained using a Jobin–Yvon T 64000 spectrophotometer. The scattering intensities of films were measured using an Aminco-Bowman series-2 luminescence spectrometer with a solid film holder. Photocurrent–voltage curves were measured using a Keithley Model M236 source measure unit. A 300 W Xe lamp with an AM 1.5 filter (Oriel) was used to illuminate an active area of 0.4 cm × 0.5 cm of the TiO_2 electrode at the light intensity of 1 sun (100 mW/cm^2), and an HP 8453A diode array spectrophotometer was used to estimate the amount of dye adsorbed to the TiO_2 films.

3. Results and discussion

Fig. 1a and b show representative SEM images of TiO_2 nanorods and nanotubes dried at 100 °C, respectively. Well-aligned arrays of uniform nanorods and nanotubes of diameters of ca. 180–250 nm can be seen. We emphasize that the nanostructures are of the same size, although we used different AAM pore sizes, i.e. 0.02, 0.1 and 0.2 μm. We attribute this to the fact that these sizes of commercial Whatman anodic membranes refer to the top layers of membrane (the active layers), and main body of these membranes have the same pore size of about 200 nm [16,17], as shown in Fig. 2, which also shows the cone structures of the AAM pores. Further, we observed that the diameters of these nanorods were essentially the same when annealed at above 200 °C.

Lakshmi et al. [6] mentioned that they obtained TiO_2 tubules when AAM membranes were immersed in TiO_2 sol for a brief period (5 s at 5 °C) and fibrils after immersing for 60 s at 20 °C. Zhang et al. have showed that TiO_2 nanotubes or nanorods can be obtained using a sol gel template method by changing the molar ratio of the sol [18]. We add a new dimension in this regard from the point of view of AAM pore size. We obtained predominantly nanorods, ca. 90%, with an AAM pore size of 0.1 μm, completely nanorods with 0.02 μm and nanotubes with

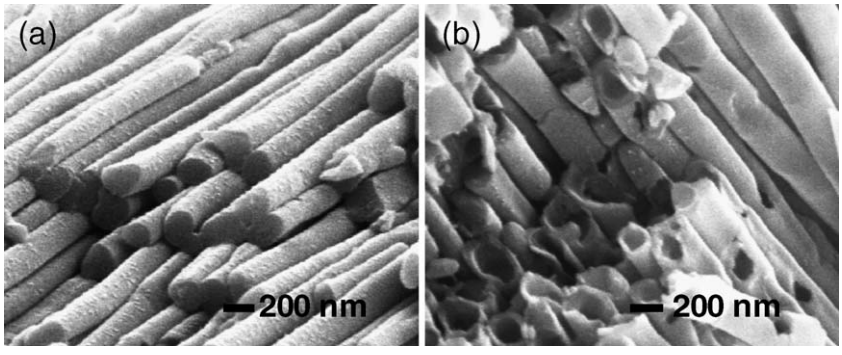

Fig. 1. SEM images of TiO_2 nanostructures produced from hydrolyzed $TiCl_4$ solutions using different pore sizes of AAM: (a) nanorods with 0.02 μm and (b) nanotubes with 0.2 μm.

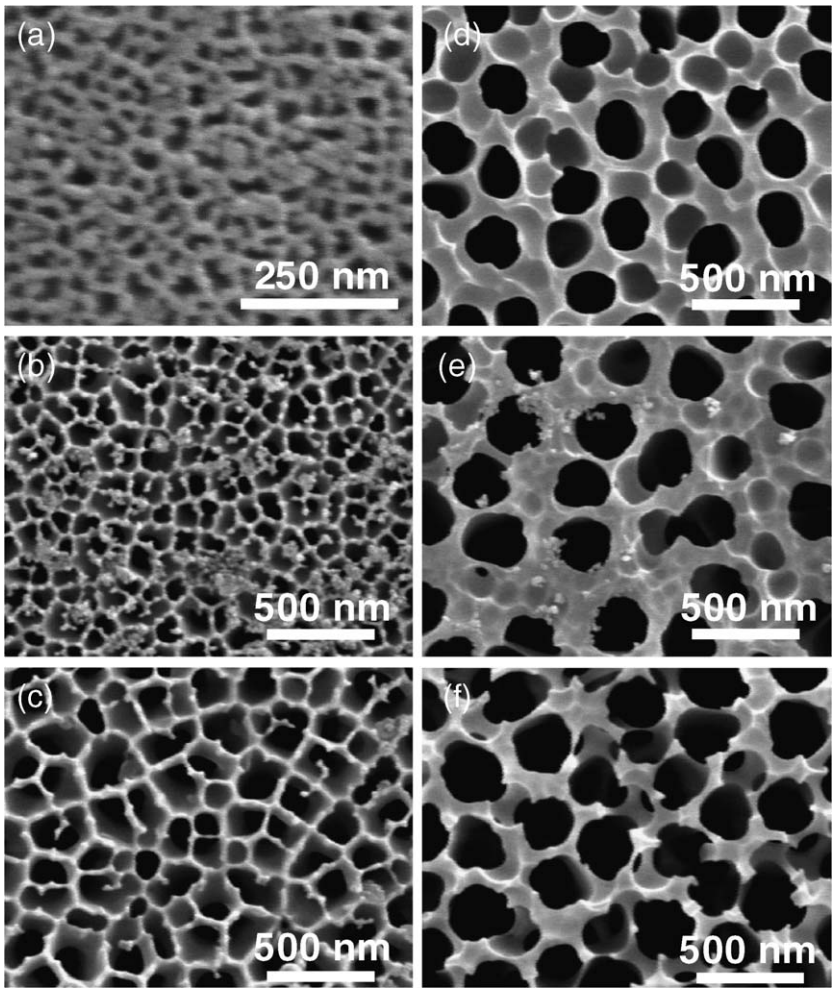

Fig. 2. SEM images of AAM pores: (a–c) are the top portions of 0.02, 0.1 and 0.2 μm pores, respectively, and (d–f) are their corresponding bottom portions, respectively.

that of 0.2 μm. These observations indicate that desired TiO_2 nanostructures can be tuned by controlling these parameters.

EDX analysis confirmed the constituents of the nanorods and nanotubes to be essentially titanium and oxygen, though traces of Cu and Na were also evident due to the copper grid used for the analysis and NaOH used for dissolution of AAM. Fig. 3 shows the Raman spectrum of TiO_2 nanorods annealed at 450 °C for 30 min. The bands are located at 144, 196 and 400 cm^{-1} (O–Ti–O bending-type vibrations) and at 517 and 638 cm^{-1} (Ti–O bond stretching-type vibrations), corresponding to the characteristic peaks of anatase TiO_2 [19]. Identical Raman spectra were obtained with nanotubes. Rutile TiO_2 is always the product from hydrolysis of $TiCl_4$. In the case of templating processes to prepare TiO_2 nanorods or nanotubes using $TiCl_4$, we have observed that the products are invariably of anatase phase [7,20,21].

Regarding the formation of TiO_2 nanostructures in AAM we propose the following mechanism: nucleation of polymeric Ti(IV) hydroxides can occur at the AAM surface. The nucleation can be initiated during heating at 50 °C, through the hydrolysis, by the formation of Ti–O–Al bonds between Ti(IV) complexes [22], such as $[Ti(OH_x)]^{(8-6x)-}$ and Al–OH sites on the pore walls [6,23]. After an initiation period, the nuclei continue to grow by attracting more Ti(IV) complexes to form partly dehydrated, polymeric Ti(IV) hydroxide particles until the neighboring particles make contact with each other to produce aggregates, leading nanostructures upon annealing.

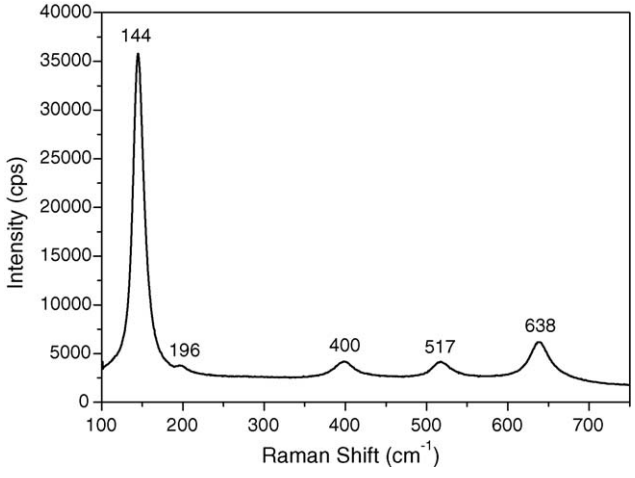

Fig. 3. Raman spectrum of anatase TiO_2 nanorods.

In the pores of the 0.02-μm AAM, the suction of hydrolyzed $TiCl_4$ by the aspirator is believed to completely fill the pores, due to the smaller upper pore size and consequent slower passage of the $TiCl_4$ solution, leading to the formation of nanorods. In the case of the 0.2-μm AAM, however, the suction facilitates passage of the $TiCl_4$ solution through larger pores, creating nanochannels in the pores, which ultimately produces nanotubes. The tubular nanostructure can withstand suction, due to its adhesion to the supporting AAM pore wall.

The question arises as to how the diameter of a single nanostructure is the same, despite the cone structure of the AAM pore. The AAM inner wall is expected to dissolve to some extent in the acidic solution of the hydrolyzed $TiCl_4$. As the $TiCl_4$ solution enters the pore wall at the surface, this surface portion is more likely to be dissolved. Because of the dissolution process at the pore mouth, the acidity of $TiCl_4$ is expected to be reduced, and thereby the internal portion of the pore is less susceptible to the acid attack. This dissolution continues during the heat treatment at 50 °C. This preferential dissolution of the pore at the template surface renders a uniform pore size from top to bottom, thereby facilitating the formation of a nanostructure of uniform diameter.

Fig. 4 shows *J–V* curves of DSSCs made by incorporating different amounts of TiO_2 nanorods into P25 film electrodes versus that of a cell fabricated with P25 only. Inset, a cross-sectional SEM image of TiO_2 film, shows nanorods (10 wt%) imbedded in a porous P25 film. Compared with the unmodified cell, the three cells incorporating 5, 10 or 15 wt% of nanorods show remarkably higher short-circuit photocurrents (J_{sc}) by about 27, 41 and 53%, respectively. The corresponding enhancements in solar energy conversion efficiencies, however, are about 27, 42 and 35%. It is clear that the increase in open-circuit voltage (V_{oc}) is small, but the same in all cases of incorporation of the nanorods. The incorporation rather reduced fill factors; for 5, 10 and 15 wt% of nanorods incorporation, the respective values are 0.62, 0.62 and 0.54, as compared to that of 0.64 for a cell without nanorods. Thus, from the point of view of solar energy conversion efficiency, 10 wt% incorporation of nanorods provided the

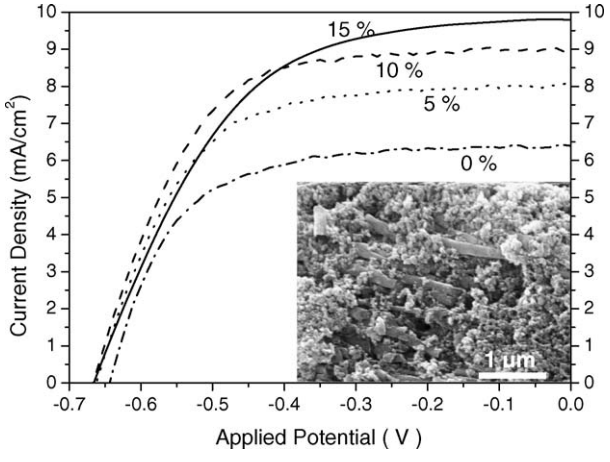

Fig. 4. *J–V* curves of DSSCs prepared with P25 film electrodes that contain different wt% of TiO_2 nanorods. Incident light intensity was 100 mW/cm^2.

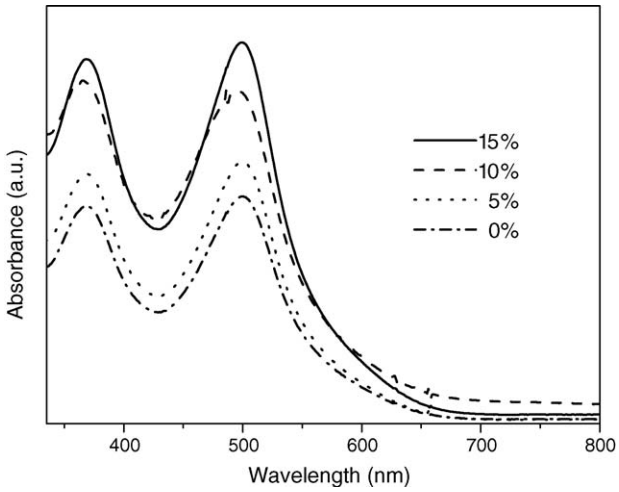

Fig. 5. Absorption spectra of dye desorbed from P25 film electrodes that contain different wt% of TiO_2 nanorods.

best DSSC performance. We have consistently observed that there is no further increase of J_{sc} above 15 wt% incorporation of nanorods.

The greatly enhanced J_{sc} is attributed to the following reasons. First, the increased surface area of films containing nanorods. These increases were found to be consistent with the amounts of dye adsorbed to TiO_2 films. Absorbance measurements of the desorbed dye from TiO_2 films with and without nanorods (Fig. 5) indicate increased dye adsorption by about 11, 33 and 48% in the case of cells with 5, 10 and 15 wt% of nanorod incorporations, respectively, compared with that of unmodified P25 film. The absorbance measurements suggest that surface areas of the TiO_2 films were increased by the incorporation of nanorods, which is in agreement with the order of J_{sc} increase.

Second, rapid electron transfer through the nanorod-incorporated film is envisaged to enhance J_{sc}. A recent analysis of intensity-modulated photocurrent spectroscopy and scanning electron microscopy data have revealed that electron transport is faster in an anatase layer than in a rutile layer [24]. P25 titania powder is composed of anatase and rutile phases. Thus, additional anatase phase content due to the added anatase nanorods facilitates higher electron transport in the film. Furthermore, DSSC photocurrent was enhanced by using single-crystalline TiO_2 nanotubes, because of a high electron transfer rate through the tubes [13b]. Using a similar experimental procedure, we established in our earlier report [4] that the lattice-plane distance of the anatase nanostructure is ca. 0.36 nm, indicating a single-crystalline nature. Thus, higher electron transport may be another reason for the higher J_{sc} of cells prepared using nanorods.

Thirdly, J_{sc} increase may also arise from enhanced light scattering by the TiO_2 films containing nanorods. Fig. 6 shows that the TiO_2 films with different contents of nanorods scatter more light at an angle of 10° over the 250–700 nm region than bare P25 film, which again is in agreement with the order of J_{sc} increase. This may be due to favorable TiO_2 cluster formation induced by the nanorods in the films.

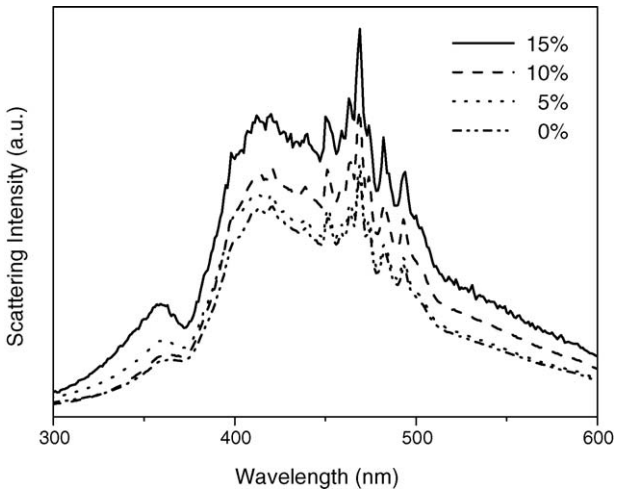

Fig. 6. Light scattering intensities of P25 film electrodes containing different wt% of nanorods, measured at 10° from light source.

Despite the increase in J_{sc} and the same V_{oc} for the cell with 15 wt% incorporation of TiO_2 nanorods, its solar energy conversion efficiency decreased versus that at 10 wt% incorporation. This is presumably caused owing to a reduction in the fill factor in the former case.

It is emphasized here that conversion efficiency is not optimized with regard to film thickness, dye purification and device architecture, as the focus of this study was on understanding the beneficial effects of AAM-regularized nanorods when added at low levels to TiO_2 film electrodes. The extrapolation of the idea of this beneficial influence in an optimized cell should render higher efficiencies.

4. Conclusions

It was observed that TiO_2 nanostructures obtained using AAMs of pore sizes 0.02, 0.1 and 0.2 μm had almost the same diameters, i.e. 180–250 nm. This is explained by the actual pore sizes in commercial Whatman AAMs. However, it was found that nanorods were obtained with pore sizes of 0.02 and 0.1 μm and nanotubes with 0.2 μm. The complete filling of smaller pores with hydrolyzed $TiCl_4$ caused by aspiration is visualized to lead to nanorods, whereas the formation of nanochannels induced by suction in the larger pores is viewed as a mechanism of nanotube formation. The greater vulnerability of the upper pore region to acid attack is viewed as the reason for the uniform diameter of a particular nanorod or nanotube, despite the cone structure of the pore. These nanostructures when added up to 10 wt% to P25 TiO_2 to make the film electrode rendered a remarkable enhancement in the shot circuit photocurrent for a DSSC and thereby in its efficiency, with slightly enhanced but the same open-circuit voltage and reduced fill factors, with respect to a cell with bare TiO_2 film electrode. The optimum level of nanorods was found to be 10 wt% from the solar energy conversion efficiency point of view. The greatly enhanced J_{sc} was found to be due to increased surface area, a higher electron transfer rate and enhanced light scattering of films containing nanorods, with respect to a bare P25 film.

Acknowledgment

This work was funded by CRM-KOSEF of Korea University and by the Sol–Gel Innovation Project.

References

[1] J. Hong, J. Cao, J. Sun, H. Li, H. Chen, M. Wang, Chem. Phys. Lett. 380 (2003) 366.
[2] F. Gracia, J.P. Holgado, A.R. González-Elipe, Langmuir 20 (2004) 1688.
[3] S.M. Liu, L.M. Gan, L.H. Liu, W.D. Zhang, H.C. Zeng, Chem. Mater. 14 (2002) 1391.
[4] I.-S. Park, S.-R. Jang, J.S. Hong, R. Vittal, K.-J. Kim, Chem. Mater. 15 (2003) 4633.
[5] P. Hoyer, Langmuir 12 (1996) 1411.
[6] B.B. Lakshmi, C.J. Patrissi, C.R. Martin, Chem. Mater. 9 (1997) 2544.
[7] P. Yang, D. Zhao, D.I. Margolese, B.F. Chmelka, G.D. Stucky, Chem. Mater. 11 (1999) 2813.
[8] R.A. Caruso, M. Giersing, F. Willig, M. Antonietti, Langmuir 14 (1998) 6333.
[9] L. Miao, S. Tanemura, S. Toh, K. Kaneko, M. Tanemura, J. Cryst. Growth 264 (2004) 246.
[10] R.A. Caruso, J.H. Schattka, A. Greiner, Adv. Mater. 13 (2001) 1577.
[11] J.-J. Wu, C.-C. Yu, J. Phys. Chem. B 108 (2004) 3377.
[12] T. Kasuga, M. Hiramatsu, A. Hoson, T. Sekino, K. Niihara, Adv. Mater. 11 (1999) 1307.
[13] (a) M. Adachi, Y. Murata, J. Takao, J. Jiu, M. Sakamoto, F. Wang, J. Am. Chem. Soc. 126 (2004) 14943;
(b) M. Adachi, Y. Murata, I. Okada, S. Yoshikawa, J. Electrochem. Soc. 150 (2003) G488.
[14] S. Ngamsinlapasathian, S. Sakulkhaemaruethai, S. Pavasupree, A. Kitiyanan, T. Sreethawong, Y. Suzuki, S. Yoshikawa, J. Photochem. Photobiol. A: Chem. 164 (2004) 145.
[15] M.G. Kang, N.-G. Park, S.H. Chang, S.H. Choi, K.-J. Kim, Bull. Korean Chem. Soc. 23 (2002) 140.
[16] Z.L. Xiao, C.Y. Han, U. Welp, H.H. Wang, W.K. Kwok, G.A. Willing, J.M. Hiller, R.E. Cook, D.J. Miller, G.W. Crabtree, Nano Lett. 2 (2002) 1293.
[17] S. Lee, C. Jeon, Y. Park, Chem. Mater. 16 (2004) 4292.
[18] M. Zhang, Y. Bando, K. Wada, J. Mater. Sci. Lett. 20 (2001) 167.
[19] T. Ohsaka, F. Izumi, Y. Fujiki, J. Raman Spectrosc. 7 (1978) 221.
[20] L. Kavan, J. Rathouský, M. Grätzel, V. Shklover, A. Zukal, J. Phys. Chem. B 104 (2000) 12012.
[21] P. Yang, D. Zhao, D.I. Margolese, B.F. Chmelka, G.D. Stucky, Nature 396 (1998) 152.
[22] Z. Yangqing, S. Erwei, C. Zhizhan, L. Wenjun, H. Xingfang, J. Mater. Chem. 11 (2001) 1547.
[23] J.W. Diggle, T.C. Downie, C.W. Goulding, Chem. Rev. 69 (1969) 365.
[24] N.-G. Park, J. van de Lagemaat, A.J. Frank, J. Phys. Chem. B 104 (2000) 8989.